



ELSEVIER

Contents lists available at ScienceDirect

Comptes Rendus Mecanique

www.sciencedirect.com



Micromechanics of granular materials – A tribute to Ching S. Chang

DEM simulations of bi-disperse ellipsoids of different particle sizes

Tang-Tat Ng^{a,b,*}, Wei Zhou^a^a State Key Laboratory of Water Resources and Hydropower Engineering Science, Wuhan University, Wuhan 430072, China^b Civil Engineering Department, University of New Mexico, NM 87131, USA

ARTICLE INFO

Article history:

Available online 26 February 2014

Keywords:

DEM

Granular materials

ABSTRACT

This paper presents the result of two schemes concerning computational effort reduction in discrete element simulations (DEM) of binary mixtures. Numerical triaxial compression simulations were performed. The coarse ellipsoids and the fine ellipsoids have similar shapes, but the sizes are significantly different. Computational effort reduction can be achieved by increasing the density of individual particles so that a greater time step can be used in DEM. Two different mass increase schemes are investigated. The result indicates that both schemes provide a speedup. Similar results can be produced with the correct damping.

© 2014 Académie des sciences. Published by Elsevier Masson SAS. All rights reserved.

1. Introduction

Real materials like sands and gravels contain particles with a wide range of sizes. To study the behavior of these multi-disperse materials using discrete element method (DEM) remains a challenge. Multi-disperse systems require tremendous computing capability. Assemblies of well-graded granular materials contain a wide range of particle sizes. As the range of particle sizes increase, the number of particles (sample size) must increase to provide a general representation. There are few numerical studies on multi-disperse systems of spheres [1,2]. The sample sizes are considerably limited since there are only a few very large particles (< 10). The behavior of these systems may not be general enough, since the largest particles can only form limited packing structures by themselves. 2-D direction shear box simulations of bi-disperse circles of various particle size ratios (diameter of large particles/diameter of small particles) indicate that the void ratio decreases with increasing particle size ratios [3].

A tremendous computational effort is required to simulate the behavior of multi-disperse systems. An attempt is made here in order to reduce the computational effort by increasing the mass. Here, we will investigate the behavior of a bi-disperse system of particles. The system contains particles of similar shapes, but different sizes. The particle size ratio (the ratio between the major axis length of the coarse particle and the major axis length of the fine particle) is 5. The mass ratio is 125. Two mass increase schemes are examined. One is the mass increase of every particle. The other method is to only increase the mass of fine particles. The results of triaxial simulations are presented.

* Tel.: +1 505 277 4844; fax: +1 505 27701988.

E-mail address: tang@unm.edu (T.-T. Ng).

2. Background

The DEM simulation time depends on sample size, time step, strain rate, contact detecting scheme, and contact updating scheme. Sample size depends on the range of particle sizes used in the simulations. The time step depends on the smallest particle size provided that the densities of the particles are the same. The strain rate depends on the initial density of the samples. Larger time steps can be used in dense samples than in loose ones. The effectiveness of contact detecting and updating schemes is affected by the range of particle sizes.

3. Time step

The time step (Δt) employed in DEM simulations is related to the square root of the ratio between the smallest mass and the greatest stiffness in the system:

$$\Delta t = bt_{\text{crit}} = b \sqrt{\frac{M_{\text{min}}}{K_{\text{max}}}} \quad (1)$$

where

b = time step constant (≤ 1)
 t_{crit} = critical time step
 M_{min} = smallest particle mass
 K_{max} = maximum stiffness at the contact between particles

The mass is a function of the particle size and of the particle density. For an ellipsoidal element of dimensions r_a , r_b , r_c , and of density ρ , $M = \rho V = \rho 4/3 \pi r_a r_b r_c$. The contact stiffness is related to the particle size by the Hertzian and Mindlin contact laws. The normal stiffness according to the Hertzian theory is given as:

$$K_n = \frac{2Ga}{1 - \nu} \quad (2)$$

where

G = shear modulus
 a = equivalent radius of contact area which is a function of normal force
 ν = Poisson's ratio

According to the Mindlin theory, the initial tangential stiffness can be related to normal stiffness as:

$$\frac{K_t}{K_n} = \frac{2(1 - \nu)}{(2 - \nu)} \quad (3)$$

For $\nu > 0$, the ratio is always less than 1. Therefore, the maximum stiffness in Eq. (1) is the maximum normal stiffness.

4. Contact detection and updating schemes

Contact detection is very time consuming in DEM simulations. To search particle contacts for all particles in every calculation cycle is not efficient. A sample is divided into sub-zones. Each sub-zone will maintain a particle list for the particles that are mapped into the sub-zone. Contact is checked only for particles listed in the same sub-zone. Depending on its size and location, a particle can be listed in more than one sub-zone. A list of possible contact pairs is created for each sub-zone. A possible contact pair is defined even for two particles that are not in contact, but whose separation is less than a threshold value. Contact calculation is performed according to the possible contact list. When the movement of particles is greater than the threshold value, both particle list and contact list will be updated. This threshold value is related to the particle size. A smaller threshold value (finer particle) implies more frequent updates of the contact list.

For a bi-disperse system of similar particle sizes (the size of coarse particles is similar to the size of fine particles), the time step is not much different from that of a mono-disperse system. A bi-disperse system of different particle sizes (the size of a coarse particle is much greater than that of a fine particle) requires greater calculation time than that of a mono-disperse system of coarse particles only. In addition, the time spent in contact detection in such a bi-disperse system is also greater than that with a mono-disperse system. In addition, the updating scheme is not as efficient as that of a system with similar particle sizes. 2-D studies on contact detection of a system of different particle sizes have been carried out [4]. The research suggested using several grid sizes instead of a single grid size for bi-disperse systems of different particle sizes. Due to the nature of their particular simulations (problems of rotating drum and silos), the study did not consider the use of contact list. In our study of granular materials, the contact list can significantly reduce the time spent

in searching contact. Although the contact detection scheme is not addressed here, improvement in contact detection and updating schemes may reduce the computational effort significantly.

Reduction of simulation time can be accomplished by using either greater density or smaller stiffness (shear modulus). Using different shear moduli may result in systems of different configurations. It is difficult to produce two samples of similar configurations when different shear moduli are used. Therefore, reducing the simulation time due to shear modulus reduction is not studied here.

A previous study on bi-disperse samples of similar particle sizes with zero gravitational forces indicates that similar behaviors are observed when the parameters, including damping, time step, mass, and shear modulus vary between one-tenth of and ten-fold the corresponding benchmark value [5]. The particle mass ratio (the mass of coarse particle over the mass of fine particle) of this bi-disperse system is 1.25. The critical time step based on the fine particle is only 11% more than the critical time step based on the coarse particle. The usage of these smaller particles only increases the runtime slightly. Here, we will consider a bi-disperse system with significantly different particle sizes. The size ratio between the big particle and the small particle is 5. The critical time step based on the fine particle is more than 10 times the critical time step based on the coarse particle.

5. Numerical results

5.1. Sample preparation

A bi-disperse system of two kinds of ellipsoids is generated. The dimensions of coarse ellipsoids are 15 mm × 10 mm × 10 mm. The dimensions of fine ellipsoids are 3 mm × 2 mm × 2 mm. The particle size and mass ratios between coarse and fine particles are 5 and 125, respectively. A bi-disperse system should contain enough coarse particles. If the system contains very few coarse particles, the interaction between coarse particles is limited. Twenty-five coarse particles are chosen. A 50:50 binary mixture system (by particle mass) requires 3125 fine particles. The sample size is larger than that of the previous system (1170). The fine content of the previous system is also 50% of the total mass. From here on, we will denote this previous system as the system of similar particle sizes.

The normal contact is described using the Hertzian contact law. The initial tangential stiffness of the Mindlin's solutions is employed for the tangential contact relationship [6]. The boundaries are rigid. The interaction between particles and boundary (normal boundary force) is calculated as the product of a hydrostatic (pressure) parameter (k_p) and the intersection area between the boundary plane and the particle [7]. The properties of the elastic particles are the shear modulus of 28,957 MPa and the Poisson's ratio of 0.15. The density of the ellipsoid (ρ) is 2.65 Mg/m³. The gravity constant is reduced to 9.81 mm/s² to produce the correct unit weight of soil solid (26.0 kN/m³). The friction coefficient between particles is 0.5. The time step constant b is 0.05. These parameters are the same as those of the binary system of similar particle sizes.

Sample A is created in three steps after a random generation of particles in a rectangular prism. First (deposit phase), particles settle resulting from gravitational forces. A smaller particle–particle friction coefficient ($\mu = 0.1$) is used in this phase. The snapshots during the deposit phase are shown in Fig. 1. Second, the particle–particle friction coefficient is increased to 0.5. The system is allowed to reach the state of equilibrium. Finally, the sample is compressed to an isotropic confining pressure (100 kPa). Fig. 2 shows the final sample.

The void ratio and coordination number of Sample A are 0.478 and 4.684, respectively. The coordination number is similar to those of the systems of similar particle sizes. However, the void ratio is much lower than those of systems of similar particle sizes ($e \approx 0.69$). This is expected as smaller fine particles can fill easily in the voids form by the coarse particles. Then, the overall void ratio will decrease.

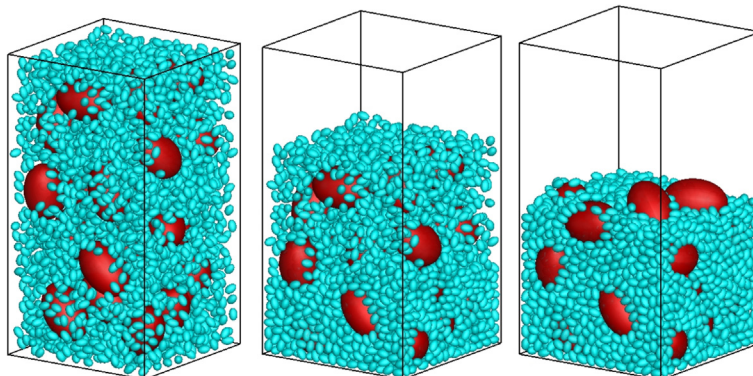


Fig. 1. (Color online.) Snapshots of the deposited phase of a sample (50% of fine content).

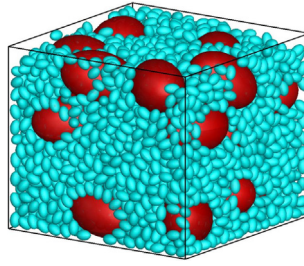


Fig. 2. (Color online.) Final configuration of Sample A.

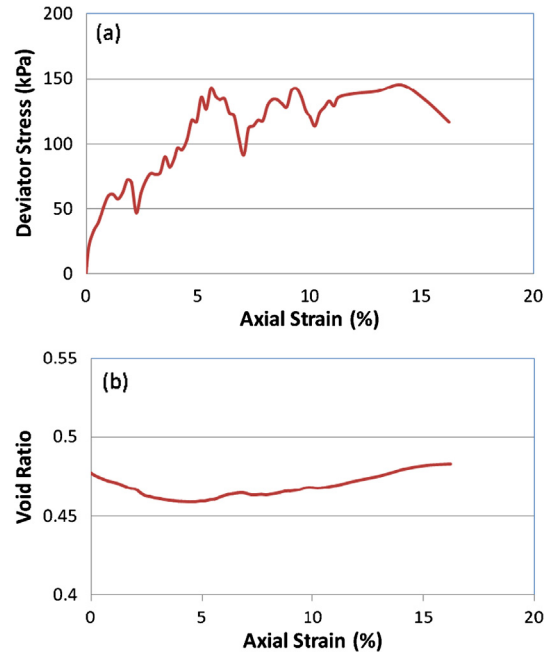


Fig. 3. (Color online.) Drained triaxial compression simulation of Sample A.

Fig. 3 shows the result of a drained triaxial compression simulation on Sample A. In the simulation, the lateral pressures remain constant at 100 kPa while the vertical stress increases. The simulation is stopped when the vertical dimension is about 60 mm (the maximum length of two aligned coarse particles). We will consider a representative bi-disperse system should have at least two coarse particles in each direction. The stress–strain curve is very jagged. It contains more ups and downs than the stress–strain curves of systems of similar particle sizes.

These ups and downs may be related to the contact force calculation at the boundaries. Since the boundary force calculation is the product of a parameter k_p ($= 10 \text{ MP}_a$) and of the intersection area, the possible intersection area of coarse particles can be 25 times greater than that of fine particles. This may affect the stability of force chains. In turns, it will affect the stress–strain curve.

5.2. Effect of hydrostatic parameter

Another sample (A1) is created by using a smaller k_p ($= 0.2 \text{ MP}_a$). The void ratios and coordination number of the final sample are 0.457 and 4.763, respectively. They are very similar to those of Sample A. The result of the triaxial simulation on Sample A1 is plotted in Fig. 4 together with the result of Sample A. A smoother stress–strain curve is seen in Fig. 4a. The general trend is similar for these two samples. If the initial void ratio of Sample A1 is the same as Sample A, the volumetric behavior will be almost identical. The difference of initial void ratio of these two systems is due to the contact area at the boundaries. The stiffness at the boundary does not affect the shape of the volumetric behavior. Therefore, the reduced parameter ($k_p = 0.2 \text{ MP}_a$) will be used in the simulations presented in this paper. Sample A1 will be used as a baseline.

Fig. 5 shows the configurations of ellipsoids and the configurations of big ellipsoids at initial state, at peak state, and at final state. The corresponding axial strains are shown in the figure. The configurations are similar, especially for the configurations of big ellipsoids.

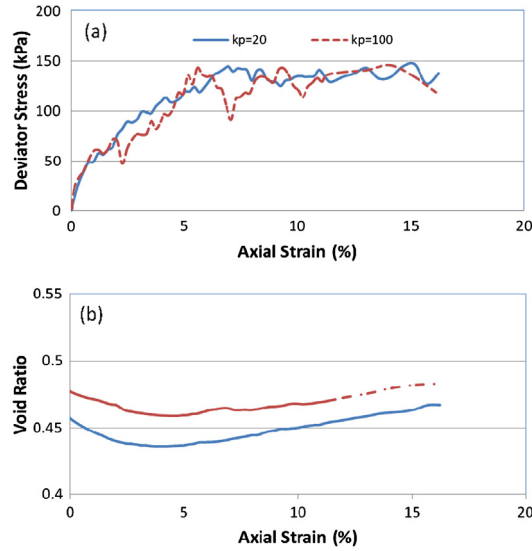


Fig. 4. (Color online.) Drained triaxial compression simulations of Samples A1 and A.

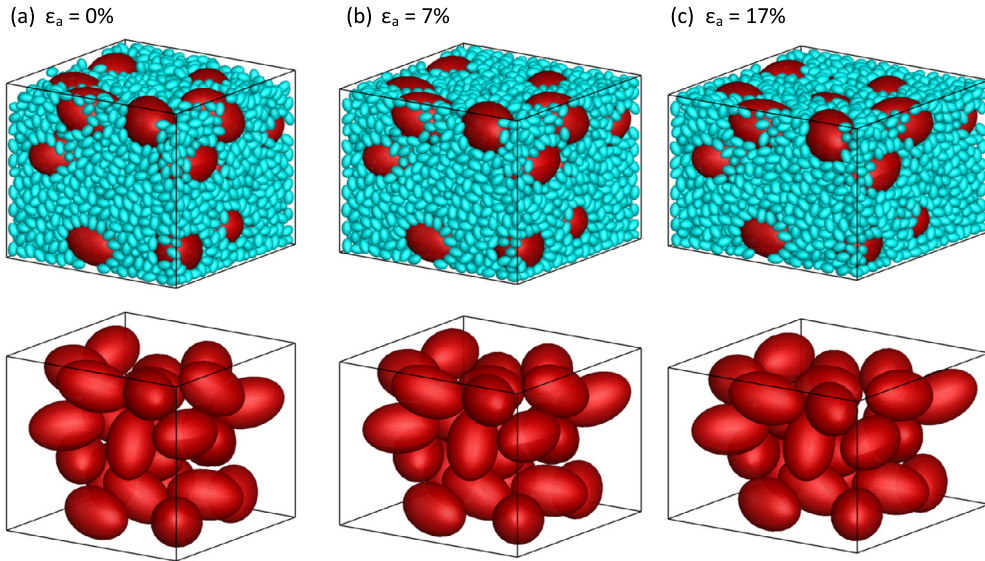


Fig. 5. (Color online.) Configurations of Sample A1 at different axial strains.

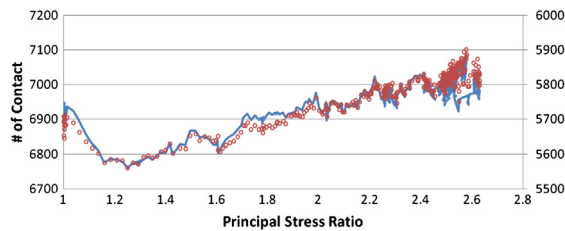


Fig. 6. (Color online.) Evolution of the number of contacts versus the principal stress ratio.

Fig. 6 shows the total number of contacts and the number of contacts between fine particles versus principal stress ratio (σ_1/σ_3). The solid curve represents the evolution of the total number of contact (plot on primary y-axis). The symbols represent the evolution of the number of contact between fine particles (plot on the secondary y-axis). As shown in Fig. 6, the total number of contacts decreases at the beginning and increases with the increase of principal stress ratio. Similar behavior can be observed for the number of contacts between fine particles. The change in the total number of contacts is

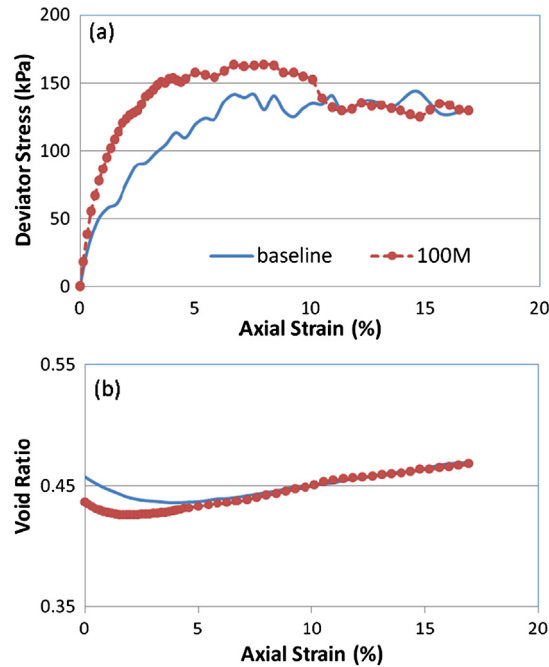


Fig. 7. (Color online.) Results of simulations with two different particle densities.

clearly related to the change between fine particles. The behavior of this bi-disperse system is dictated by the behavior of fine particles. The big particles act like rigid inclusions to transfer forces from fine particles to other fine particles that are in contact with the big particle. This may not be true when the % weight of the fine particles and particle size ratio are different. More simulations are needed to determine the general behavior of the bi-disperse system.

5.3. Reducing run time by mass increase

To explore the schemes that can speed up the simulation, we increase the density of particles by a factor of 100. The critical time step is increased by a factor of 10. The simulation can be sped up by a factor of 10. To maintain the same gravity force as that of Sample A1, the gravity constant is reduced to $9.81 \mu\text{m/s}^2$ (1/100 of the baseline). The sample preparation is the same as Sample A1. The void ratio and coordination number of Sample A2 are 0.436 and 4.670, respectively. The void ratio and the coordination number are less than those of Sample A1. It indicates that the configuration of Sample A2 is different from that of Sample A1. The effect of the gravity constant is evident. These two samples start with the same initial potential energy. The kinetic energy and the energy dissipation due to damping during the deposit process are different. Greater mass increases the amount of damping when the same user defined constant α is used. In DEM simulations, a mass proportional Rayleigh damping is:

$$c = \alpha m \quad (4)$$

Fig. 7 shows the drained triaxial compression simulation of Sample A2 together with Sample A1. The solid curve represents the baseline simulation ($\rho = 2.65 \text{ Mg/m}^3$). The symbols are the simulation with an elevated mass (100 M). Greater initial stiffness and higher peak strength are found for Sample A2. It is due to the greater initial density of this sample. Although the simulation stops before 40% (the general strain where critical state is reached for systems of similar particle sizes), the trend clearly shows that the critical void ratio and critical shear strength of Samples A1 and A2 are similar. The use of an elevated mass in numerical simulations does not affect the determination of the critical state.

If we start with the final configuration of Sample A1 (see Fig. 2), we perform the simulation with a reduction of the gravity constant and an increase of the particle density ($\rho = 265 \text{ Mg/m}^3$). The mass of the particles is 100 times the original value. The result is shown in Fig. 8. Greater shear strength and dilation are observed due to the increase of the mass. A previous study of systems with similar particle sizes has shown that a similar behavior is obtained as long as the damping remains within a certain range [5]. However, when damping is above this range, greater shear strength and dilation are observed.

The damping ratio of a system can be defined as:

$$\beta = c/c_{\text{crit}} \quad (5)$$

where c_{crit} is critical damping of the system:

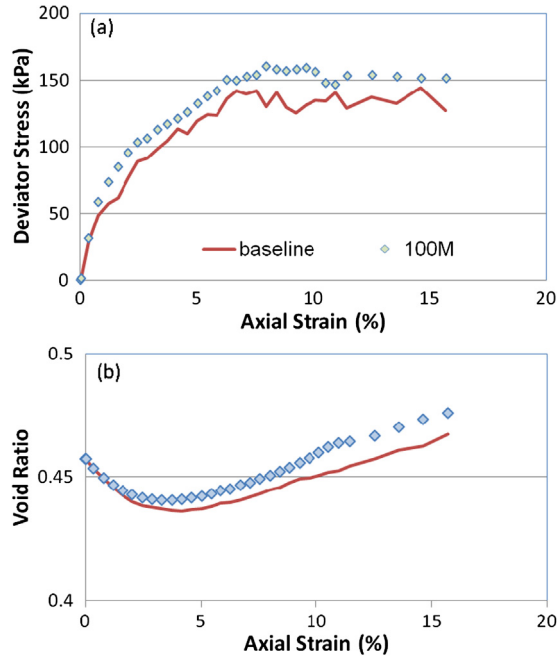


Fig. 8. (Color online.) Results of compression simulations with two different particle densities.

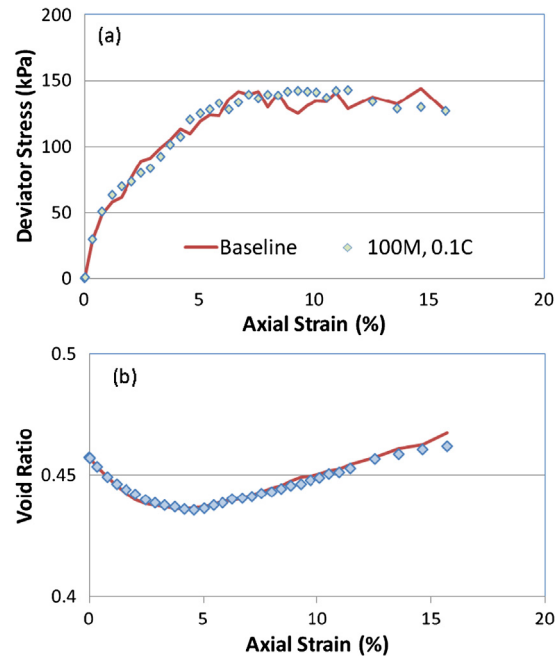


Fig. 9. (Color online.) Effect of mass increase and damping reduction.

$$c_{\text{crit}} = 2m\omega_n \tag{6}$$

Considering the simple vibration system between two particles in DEM, the natural frequency can be related to the critical time step. β can be in terms of the critical time step as:

$$\beta = 0.5 \times \alpha / \omega_n \propto \alpha \times t_{\text{crit}} \tag{7}$$

To investigate the effect of the increase of β due to the use of an elevated mass α is reduced to 1/10 of the baseline value since the critical time step increases tenfold due to the mass increase. A simulation with damping reduction is shown in Fig. 9 together with the baseline simulation. By reducing the damping (two systems have the same damping ratio), the

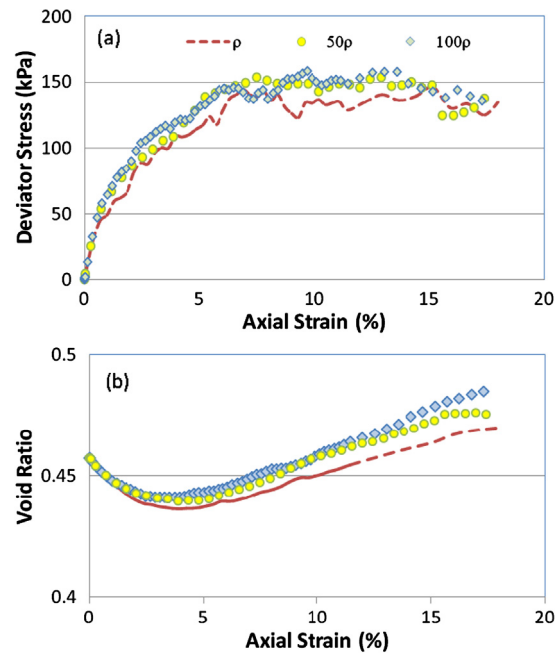


Fig. 10. (Color online.) Results of simulations with different densities of fine particles.

results of two simulations are almost identical. Therefore, it is possible to reduce the runtime by increasing the mass of the particles. Past experience of DEM simulations has indicated that when damping remains within a certain range, similar results have been observed. Therefore, to avoid the effect of damping, simulations with elevated mass can be used when damping ratio is similar to that of the baseline simulation.

5.4. Mass increase of fine particles

Another way to speed up the simulation is to artificially increase the density and reduce the gravity constant of fine particles, but not of the coarse particles. Two densities are used for the fine particles, i.e. 132.5 Mg/m^3 (50ρ) and 265 Mg/m^3 (100ρ). The calculation time can be reduced by 1/7 and 1/10 due to the increase of critical time step. To keep the same gravitational forces, the corresponding gravity constant of fine particles is reduced accordingly. The gravity constant of coarse particles remains unchanged. Fig. 10 shows the results together with those obtained with Sample A1 (baseline). Similar behaviors are observed for these three simulations. A slightly higher shear strength and a greater dilation are found when using greater mass. This is the effect of the increase of mass damping.

To maintain the same damping ratio (see Eq. (7)), a simulation is carried out with the elevated density of fine particles (100ρ) and the damping (C) is reduced by 1/10. Fig. 11 shows the result together with the baseline. The result is almost identical. Therefore, it is possible to reduce the runtime and produce the baseline result with the technique of density increase of fine particles as long as the correct damping is used.

Fig. 12 shows the comparison between the simulation with elevated mass (100ρ) and the simulation with elevated mass for fine particles only (100ρ). Damping is adjusted to the value used in the baseline simulation. The results are very similar. The general mass increase scheme (solid curve) provides a smoother stress–strain curve. For this particular sample, both schemes are acceptable. However, it is expected that the two schemes may provide different results in some cases. Further investigation is needed. Care must be taken when using these schemes.

In the simulation with reduced mass, the time step is increase ten-fold compared to that used in the simulation of regular masses. Can we use this high time step in the simulation with regular masses? Previous study of the time step has shown that the time step constant should be below 0.2 for meaningful results [5]. A baseline simulation with a time step constant of 0.5 is carried out accidentally. The stress–strain behavior is shown in Fig. 13 together with the simulation of elevated masses. The volumetric behavior is almost identical. The simulation with elevated masses produces a smoother stress–strain curve. Using a greater time step for this particular system looks possible. Reduction of computing time can be accomplished by using a greater time step although a jagged stress–strain curve is developed. Researchers have to be careful since past experiments had indicated that using such a high time step (0.5) did not work in many numerical simulations.

Reducing the computational effort is possible, but care has to be taken. This preliminary study has shown that the reducing scheme can be case-dependent. Until a consistent trend is discovered, it is recommended that a similar study should be preformed for any new simulation on the reduction of the computational effort.

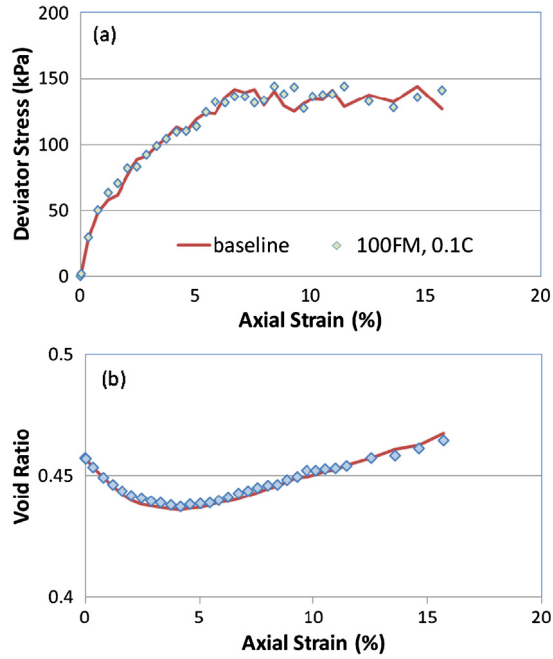


Fig. 11. (Color online.) Results of simulations with different damping ratios.

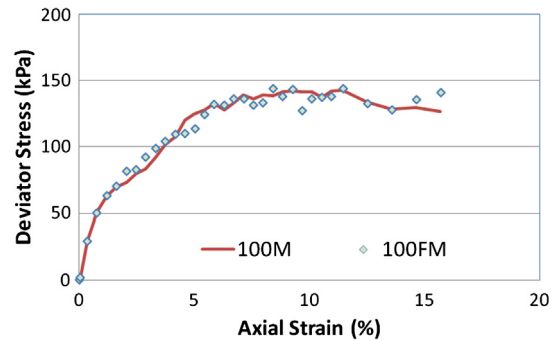


Fig. 12. (Color online.) Results of simulations with two different mass increase schemes.

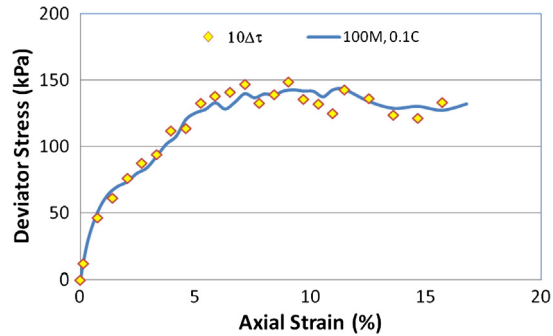


Fig. 13. (Color online.) Results of two simulations with the same time step but different masses.

6. Conclusions

Simulations of samples of two kinds of ellipsoids with significant size difference have been carried out. A parameter used in the simulations of samples of ellipsoids of similar size needs to be modified to produce a smooth stress–strain curve. For a sample with 50% of fine content, the behavior is dominated by the fine particles, as expected. This domination is observed through the movement of fine particles and the contact information between fine particles.

Reduction of runtime has been attempted by increasing the mass (density) of the fine particles alone or the mass of all particles. Also, it can be accomplished by using a greater time step. Without the correction of damping, simulation of elevated masses shows higher shear strength and greater dilation. Further investigation of damping indicates that the baseline behavior can be reproduced when correct damping is used in the simulation of elevated masses. Damping must be applied in such a way that the damping ratio of the system is similar to the baseline. There is no difference in elevating the mass of fine particle alone or elevating the mass of every particle, although the general elevated mass scheme produces a smoother stress–strain curve.

The paper has reported a preliminary study on the reduction of the computational effort of one sample. More simulations should be carried out to provide general conclusions.

Acknowledgements

The authors would like to thank the reviewers for their comments that helped to improve the manuscript. The research effort has been partially supported by Wuhan University.

References

- [1] T.G. Sitharam, M.S. Nimbkar, Micromechanical modeling of granular materials: Effect of particle size and gradation, *Geotech. Geol. Eng.* 18 (2000) 91–117.
- [2] C. Clauquin, F. Emeriault, Interface behavior of granular materials: discrete numerical simulation of a ring simple shear test, in: *Proc. 15th Engineering Mechanics Conference*, 2–5 June 2002, New York, 2002.
- [3] T. Ueda, T. Matsuhima, Y. Yamada, Effect of particle size ratio on shear strength of dense binary mixtures, in: M. Jiang, F. Liu, M. Bolton (Eds.), *Geomechanics and Geotechnics: From Micro to Macro*, 2001, pp. 507–511.
- [4] H. Mio, A. Shimosaka, Y. Shirakawa, J. Hidaka, Optimum cell size for contact detection in the algorithm of the discrete element method, *J. Chem. Eng. Jpn.* 38 (12) (2005) 969–975.
- [5] T.-T. Ng, Input parameters of discrete element method, *J. Eng. Mech.* 132 (7) (2006) 723–729.
- [6] X. Lin, T.-T. Ng, A three-dimensional element model using arrays of ellipsoids, *Geotechnique* 47 (2) (1997) 319–329.
- [7] T.-T. Ng, Hydrostatic boundaries in discrete element methods, in: *Discrete Element Methods: Numerical Modeling of Discontinua*, in: *Geotechnical Special Publication*, vol. 117, ASCE, 2002, pp. 47–51.